FAM109B plays a tumorigenic role in low-grade gliomas and is associated with tumor-associated macrophages (TAMs)

Zhe Zhang[1,2,3,4†], Yao Xiao[1,2,3,4†], Siyi Zhao[1†], Jun Liu[1], Jie Zeng[1,2,3,4], Feng Xiao[1,2,3,4], Bin Liao[1,2,3,4], Xuesong Shan[1], Hong Zhu[1,2,3,4*] and Hua Guo[1,2,3,4*]

Abstract

Background Family with sequence similarity 109, member B (FAM109B) is involved in endocytic transport and affects genetic variation in brain methylation. It is one of the important genes related to immune cell-associated diseases. In the tumor immune system, methylation can regulate tumor immunity and influence the maturation and functional response of immune cells. Whether FAM109B is involved in tumor progression and its correlation with the tumor immune microenvironment has not yet been disclosed.

Methods A comprehensive pan-cancer analysis of FAM109B expression, prognosis, immunity, and TMB was conducted. The expression, clinical features, and prognostic value of FAM109B in low-grade gliomas (LGG) were evaluated using TCGA, CGGA, and Gravendeel databases. The expression of FAM109B was validated by qRT-PCR, immunohistochemistry (IHC), and Western blotting (WB). The relationship between FAM109B and methylation, Copy Number Variation (CNV), prognosis, immune checkpoints (ICs), and common chemotherapy drug sensitivity in LGG was explored through Cox regression, Kaplan–Meier curves, and Spearman correlation analysis. FAM109B levels and their distribution were studied using the TIMER database and single-cell analysis. The potential role of FAM109B in gliomas was further investigated through in vitro and in vivo experiments.

Results FAM109B was significantly elevated in various tumor types and was associated with poor prognosis. Its expression was related to aggressive progression and poor prognosis in low-grade glioma patients, serving as an independent prognostic marker for LGG. Glioma grade was negatively correlated with FAM109B DNA promoter methylation. Immune infiltration and single-cell analysis showed significant expression of FAM109B in tumor-associated macrophages (TAMs). The expression of FAM109B was closely related to gene mutations, immune checkpoints (ICs), and chemotherapy drugs in LGG. In vitro studies showed increased FAM109B expression in LGG, closely related to cell proliferation. In vivo studies showed that mice in the sh-FAM109B group had slower tumor growth, slower weight loss, and longer survival times.

Conclusions FAM109B, as a novel prognostic biomarker for low-grade gliomas, exhibits specific overexpression in TAMs and may be a potential therapeutic target for LGG patients.

---

†Zhe Zhang, Yao Xiao and Siyi Zhao contributed equally to this work.

*Correspondence:
Hong Zhu
zhuzuhongzhuzuhong@outlook.com
Hua Guo
ndefy02014@ncu.edu.cn
Full list of author information is available at the end of the article

Zhang *et al. Journal of Translational Medicine*   (2024) 22:833

Page 2 of 15

Introduction

Gliomas are the most common primary central nervous system (CNS) tumors, with the highest incidence and mortality rates among CNS tumors in both children and adults [1, 2]. Gliomas can be classified into main types such as oligodendrogliomas, astrocytomas, glioblastomas, and mixed gliomas [3]. According to the 2016 World Health Organization (WHO) classification, gliomas are divided into high-grade gliomas and low-grade gliomas. Diffuse low-grade gliomas (WHO grade II) and intermediate gliomas (WHO grade III) are classified as low-grade gliomas (LGG), including astrocytomas, oligoastrocytomas, and oligodendrogliomas [4, 5]. As understanding of low-grade gliomas improves and diagnostic and therapeutic techniques for low-grade gliomas advance, the prognosis of LGG patients is generally better than that of high-grade gliomas (HGG) [6]. However, recurrence and malignant progression leading to high-grade gliomas remain the main causes of poor prognosis in low-grade glioma (LGG) patients [7]. Therefore, it is necessary to study the factors influencing the malignant progression of low-grade gliomas in depth, develop new therapeutic targets, and provide more precise treatment to effectively improve patient prognosis.

Family with sequence similarity 109, member B (FAM109B) is involved in endocytic transport and affects genetic variation in brain methylation, playing a pleiotropic role in psychiatric disorders [8, 9]. FAM109B is closely related to the occurrence of Alzheimer's disease and schizophrenia [10]. It is also closely associated with Lowe (OCRL) syndrome, a rare genetic disease that mainly affects the brain [11]. Additionally, FAM109B is sensitive to drugs in breast cancer cell lines and shows sensitivity to radiation [12]. FAM109B participates in certain neurological diseases through genetic variation, but its expression and prognostic significance in common CNS tumors are unknown. Summary-based mendelian randomization (SMR) analysis has identified FAM109B as an important immune cell-related disease gene [13], but it is unclear how FAM109B affects immune cell function and tumor immune cell infiltration. The tumor microenvironment (TME) influences tumor cell progression and metastasis, as well as resistance to anticancer drugs, playing a crucial role in tumor development [14, 15]. However, the relationship between FAM109B and the tumor microenvironment remains unclear.

In this study, we conducted bioinformatic analysis using the TCGA, Gravendeel, and Chinese Glioma Genome Atlas (CGGA) datasets to determine the potential of FAM109B as a biomarker for glioma prognosis and immunotherapy. For the first time, we revealed the expression, immune infiltration, and prognostic significance of FAM109B across 33 types of cancer. We explored the correlation between FAM109B and low-grade gliomas in terms of tumor malignant progression, DNA methylation, single-cell transcriptomics, CNV, chemotherapy efficacy, and immunological characteristics (immune checkpoint gene expression, tumor-infiltrating immune cells). Through in vitro and in vivo experiments, we suggest that FAM109B could be a prognostic factor for LGG patients and may become a new therapeutic target for LGG in future clinical practice.

Materials and methods

Data collection

Pan-cancer information (33 types of cancer), mRNA-seq, clinical characteristics, and tumor mutation burden (TMB) data from The Cancer Genome Atlas (TCGA) dataset and GTEx dataset were obtained from UCSC Xena [16]. The Chinese Glioma Genome Atlas (CGGA) dataset [17] and Gravendeel dataset [18], including mRNA-seq and clinical information of patients, were downloaded to analyze the expression and prognostic potential of FAM109B in LGG. The inclusion criteria were patients with WHO grade II or III and complete prognostic information, comprising 531 patients from the TCGA dataset, 257 patients from the CGGA dataset, and 109 patients from the Gravendeel dataset. This study was approved by the Ethics Review Committee of the Second Affiliated Hospital of Nanchang University (Project approval ID: O-Medical Research Ethics Review 【2024】 No. 21). The study flowchart is shown in Fig. 1.

Prognostic analysis

Overall survival (OS), disease-specific survival (DSS), and progression-free interval (PFI) were analyzed, with $p < 0.05$ considered statistically significant. Univariate and multivariate Cox regression analyses were used to investigate the relationship between FAM109B expression and survival outcomes. Receiver operating characteristic (ROC) curves and the area under the curve (AUC) were used to assess the accuracy of FAM109B expression in predicting LGG prognosis.
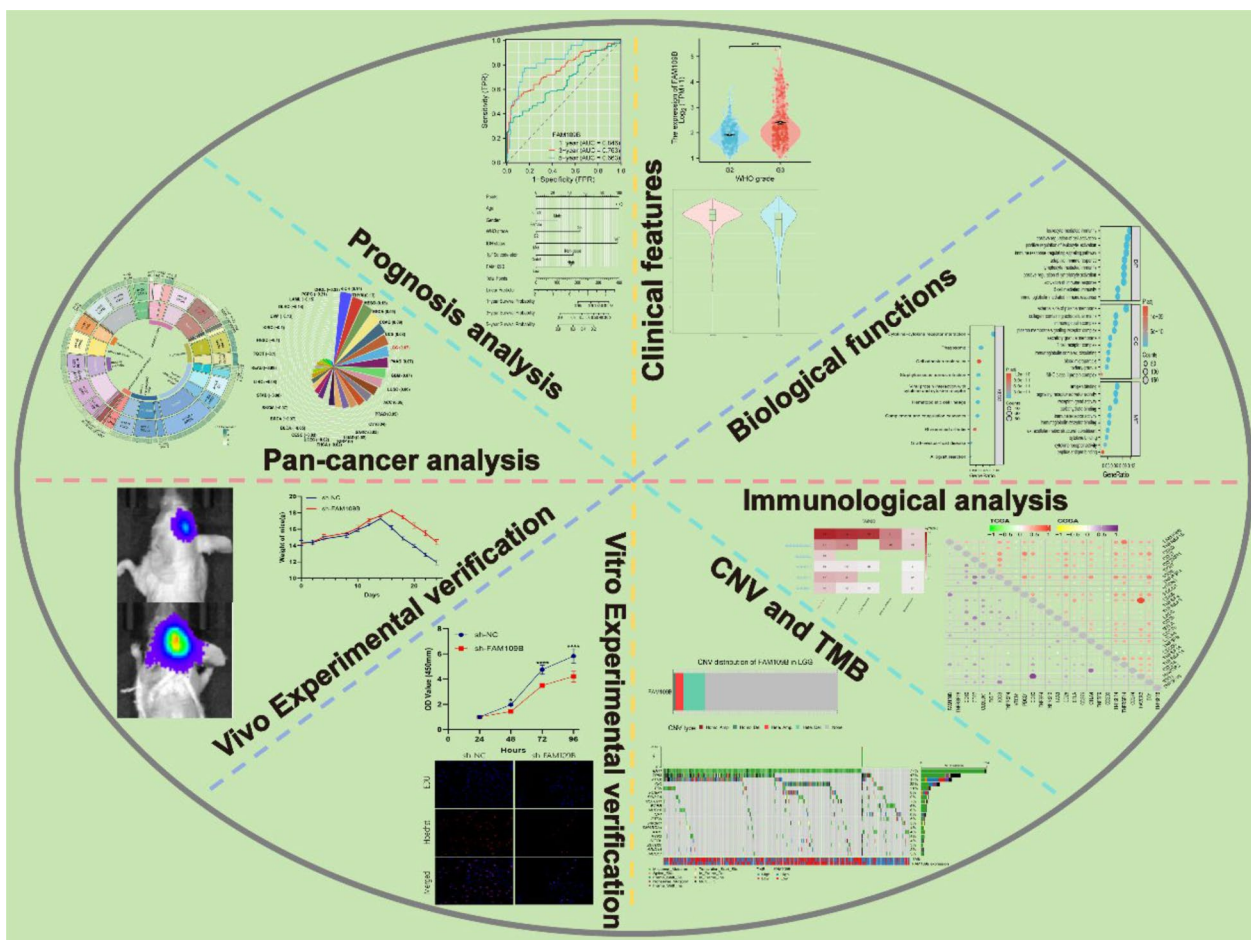
Fig. 1 Schematic diagram of the research content. It includes pan-cancer analysis, clinical features analysis, prognosis analysis, biological functions, immunological analysis, CNV and TMB analysis, in vitro experimental and in vivo experiment

Immunohistochemistry and immunofluorescence staining

The Human Protein Atlas (HPA) was used to analyze the differential expression of FAM109B between normal and glioma tissues [19]. Tissue samples from 9 low-grade glioma patients and 3 normal brain tissues treated at the Neurosurgery Department of the Second Affiliated Hospital of Nanchang University from 2020 to 2023 were collected and embedded in paraffin. FAM109B expression was detected using IHC. According to the manufacturer's instructions, 5 μm thick sections were deparaffinized, hydrated, and fully immersed in 3% hydrogen peroxide solution, incubated for 10 min, then rinsed with running water for 5 min. Staining was performed with anti-FAM109 (1:500, sc-390442), followed by dehydration, clearing, and mounting. Finally, the IHC results were evaluated under a microscope by two intermediate pathologists. The tumor specimens of nude mice were fixed with 4% paraformaldehyde. After incubation with the primary antibody CD163 (1:1000, ab182422, Abcam), the sections were treated with Fluor-594 secondary

antibody (1:1000, ab150080, Abcam) for 1 h and stained with Hoechst 33258 (94403, Sigma) solution for 5 min. Finally, they were washed with PBS to remove excess dye and photographed using a confocal laser scanning microscope.

Western blotting and quantitative real-time PCR (qRT-PCR)

The collected brain tissue samples were obtained from the Department of Neurosurgery at the Second Affiliated Hospital of Nanchang University. Proteins were separated using 12% SDS-PAGE and transferred to a PVDF membrane (Millipore, USA). The membrane was incubated with antibodies targeting FAM109B (1:500, sc-390442) and α-tubulin (1:4000; 11224-1-AP), followed by incubation with the corresponding secondary antibodies. Membrane imaging was performed using the Tanon (5200Multi) imaging system, and the protein band intensity was quantified using Image J. Total RNA was extracted from the tissues using Simply P Total RNA Extraction (BioFluX, Shiga, BSC52M1), and the isolated

Zhang *et al. Journal of Translational Medicine*   (2024) 22:833

Page 4 of 15

RNA quantity was measured using MonAmp RapidStart Universal SYBR Green qPCR Mix (Monad, MQ10701S). The primers for FAM109B were forward 5′-TGGCTA CATGCGCCTGGTG-3′ and reverse 5′-GAGCCTGGG GCTTACAGCG-3′.

Establishment and validation of the clinical nomogram model

In the TCGA dataset, a clinical nomogram model was established using the "survival" and "rms" R packages, and a calibration curve was generated. The same method was used for validation in the CGGA dataset.

DNA methylation analysis

The MethSurv database was used to analyze the methylation levels of FAM109B and the prognostic significance of individual CpGs in gliomas [20].

Functional enrichment analysis

Differentially expressed genes (DEGs) of FAM109B were analyzed in the TCGA and CGGA datasets using the "limma" R package (p < 0.05 and |logFC| ≥ 1) [21]. Gene Ontology (GO) and Kyoto Encyclopedia of Genes and Genomes (KEGG) enrichment analyses were performed using the "clusterProfiler" R package.

Immune analysis and single-cell analysis

The TIMER database was used to evaluate the relationship between FAM109B and immune cell infiltration [22]. The ssGSEA algorithm provided in the "GSVA" R package was used to calculate the immune infiltration of 24 types of immune cells [23, 24]. Single-cell analysis was performed using the TME-related TISCH2 database [25]. Pearson correlation analysis was conducted to evaluate the relationship between FAM109B expression and markers of macrophage M1 and M2 subtypes in the TCGA and CGGA databases.

Copy number variation (CNV) and chemotherapy drug evaluation analysis

GISTIC 2.0 was used to process the CNV data of 11,495 samples downloaded from the TCGA database, identifying significantly altered regions of amplification or deletion in the low-grade glioma patient group and determining the copy number levels and prognostic significance of FAM109B [26]. The correlation between FAM109B expression and drug IC50 was analyzed using drug sensitivity data and mRNA expression data from the Genomics of Therapeutics Response Portal (CTRP, 481 small molecules in 1001 cell lines) and the Genomics of Drug Sensitivity in Cancer (GDSC, 265 small molecules in 860 cell lines), displaying the top 30 drugs [27].

Cell culture and transfection

The U251 glioma cell and SW1088 low-grade glioma cell line were obtained from the American Type Culture Collection. Cells were cultured in L-15 medium containing 10% fetal bovine serum (Gibco) at 5% CO_2 and 37 °C. SW1088 cells were transfected with lentiviral vectors containing FAM109B shRNA (5′-GCTCATCCTGGA AGTCTGTTG-3′) and negative control (NC) at a multiplicity of infection of 10.

Colony formation assay, cell counting kit-8 (CCK-8) assay, EdU assay

Cells were incubated in 6-well plates at 2×10^3 cells per well for 14 days. Cells were fixed with 4% paraformaldehyde and stained with 0.1% crystal violet staining solution, followed by quantification of the colony numbers. Transfected cells were seeded in 96-well plates (2×10^3 cells/well), incubated for 24 h, 48 h, 72 h, and 96 h. Cell proliferation was assessed using the Cell Counting Kit-8 assay (Glpbio) by measuring optical density (OD) levels according to the manufacturer's instructions. Transfected cells were seeded in 24-well plates (2×10^4 cells/ well) and incubated for 3 days before being treated with EdU reagents. SW1088 cells infected with luciferase were fluorescence assays by IVIS. Cells were fixed with 4% paraformaldehyde and 0.5% Triton X-100, stained with Hoechst dye, and EdU incorporation rates were calculated using ImageJ.

In Vivo tumor model in nude mice

Four-week-old BALB/c male nude mice were purchased from China Extractive Medicine Kang Company. U251-sh-NC and U251-sh-FAM109B cells (5×10^5) were implanted into the brains of nude mice using a stereotactic device (RWD Life Science, Shenzhen, China) to establish intracranial tumor models (n = 5 per group). Tumor formation and size were confirmed and evaluated on days 0, 7, 14, and 21 using an IVIS spectrum real-time imaging system (Branford, USA), with corresponding body weight changes recorded. This study was approved by the Experimental Animal Ethics Committee of Nanchang University (No. NCULAE-20221031035).

Statistical analysis

Data analysis was primarily performed using R (V 4.1.2), SPSS (V26.0), and GraphPad Prism (V 8.0). The "stats" and "car" R packages were used to analyze the correlation between FAM109B and clinical characteristics. Survival prognosis was evaluated using Kaplan–Meier curves. Cox regression analysis was employed to assess independent prognostic factors. The significance of differences was tested using Student's t-tests. Correlations between

variables were tested using Pearson or Spearman correlation tests. Differences were considered significant at *p < 0.05, **p < 0.01, ***p < 0.001, and ****p < 0.0001.

Results

Pan-cancer analysis of FAM109B expression

We explored the expression of FAM109B mRNA, by integrating various types of cancer databases (TCGA) and normal tissue databases (GTEx) (Fig. 2B). FAM109B was upregulated in BRCA, CHOL, DLBC, GBM, HNSC, KIRP, LAML, LGG, LIHC, LUAD, OV, PAAD, PCPG, SKCM, TGCT, and THYM. However, it was downregulated in ACC, ESCA, KICH, LUSC, THCA, UCEC, and UCS (Fig. 2A). Subsequently, we analyzed the correlation between FAM109B expression and 22 common immune infiltrating cells in 33 types of tumors. FAM109B was closely associated with macrophages in ACC, BLCA, BRCA, COAD, DLBC, GBM, HNSC, KIRC, KIRP, LAML, LGG, LIHC, LUAD, LUSC, OV, PCPG, PRAD, READ, SARC, SKCM, STAD, TGCT, THCA, THYM, UCS, and UVM (Fig. 2C). Additionally, we analyzed the correlation between FAM109B expression and TMB. In KICH, THYM, MESO, ESCA, COAD, UCS, LGG, PAAD, GBM, LUSC, ACC, PRAD, OV, SARC, and LUAD, FAM109B expression was positively correlated with TMB levels (Fig. 2D).

To examine the prognostic significance of FAM109B expression in 33 types of tumors, we evaluated the correlation between FAM109B expression and OS, PFI, and DSS. Univariate Cox regression analysis showed that FAM109B was a risk factor for OS in BLCA, LAML, LGG, and MESO (Supplementary Fig. 1A). Kaplan–Meier curves indicated that elevated FAM109B expression was significantly associated with reduced OS in BLCA, LAML, LGG, and MESO (Supplementary Fig. 1A). Cox regression analysis of PFI indicated that FAM109B was a risk factor for BLCA, LGG, and TGCT, while it was a protective factor in KIRP (Supplementary Fig. 1B). Kaplan–Meier curves showed that elevated FAM109B expression was associated with reduced Survival probability in BLCA, LGG, and TGCT, but extended Survival probability in KIRP (Supplementary Fig. 1B). Furthermore, DSS Cox regression analysis showed that FAM109B was a risk factor for GBM and LGG (Supplementary Fig. 1C). Similarly, Kaplan–Meier curves indicated that elevated FAM109B levels were associated with poor prognosis in GBM and LGG (Supplementary Fig. 1C).
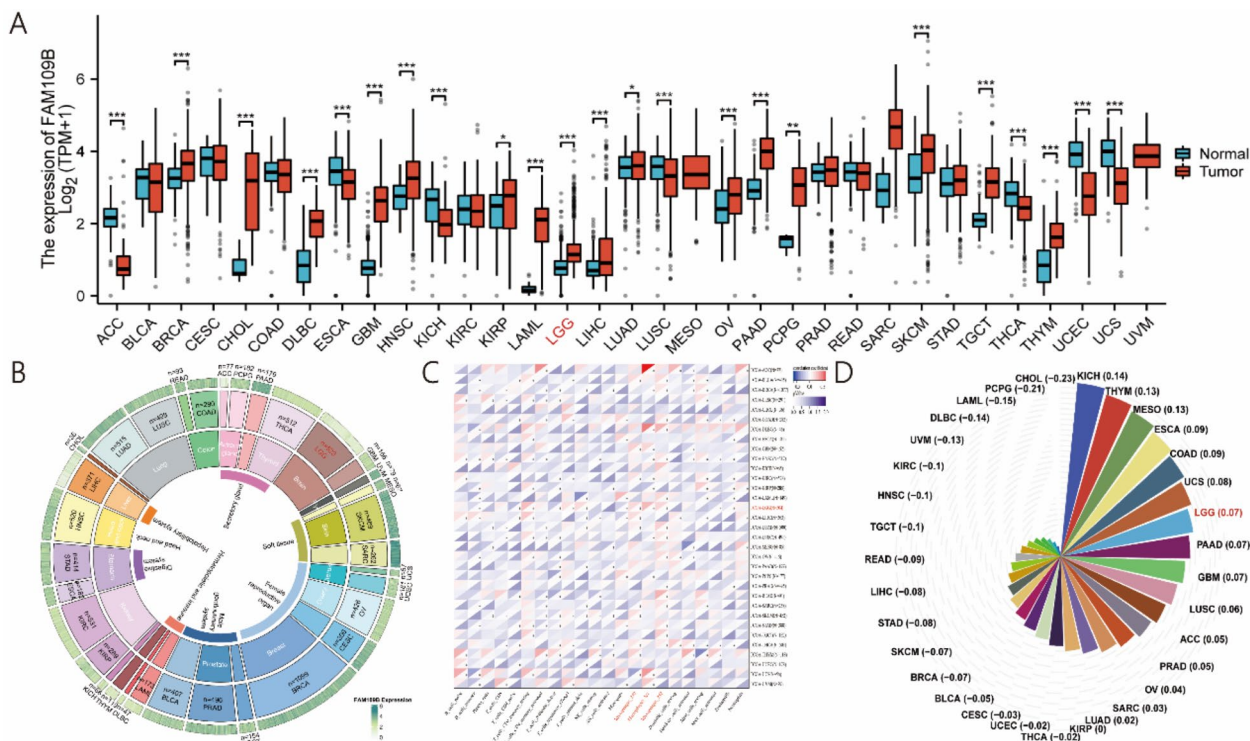

Fig. 2 Comprehensive pan-cancer analysis of FAM109B. **A** Expression of FAM109B in tumor tissues and corresponding normal tissues across 33 types of cancer. **B** Expression of FAM109B in the pan-cancer dataset. Differences in immune infiltrating cells (**C**) and TMB (**D**) across different tumors. *p < 0.05, **p < 0.01, and ***p < 0.001

Zhang *et al. Journal of Translational Medicine*   (2024) 22:833

Page 6 of 15

Correlation between FAM109B expression and clinical features in LGG

Through the analysis of the Gravendeel database, we confirmed that FAM109B is highly expressed in LGG (Supplementary Fig. 2A). In order to verify the accuracy of FAM109B expression, we further evaluated the levels of FAM109B in tissue samples from patients with low-grade glioma using qPCR, immunohistochemistry, and WB methods. Based on the cohort of patients from the Neurosurgery Center of the Second Affiliated Hospital of Nanchang University, qRT-PCR results showed that FAM109B was significantly upregulated in low-grade glioma tissues (n=9) compared to normal brain tissues (n=3) (Supplementary Fig. 2B). Immunohistochemical staining was significantly positive in LGG patients compared to normal brain tissues (Supplementary Fig. 2G). The protein expression of FAM109B in LGG tissues was higher than that in normal tissues (Supplementary Fig. 2D, n=3). The qPCR, WB results, and HPA database findings were consistent, indicating that FAM109B is significantly enriched in glioma tissues compared to normal tissues (Supplementary Fig. 2F). We analyzed the relationship between FAM109B expression levels in LGG and clinical features such as age, gender, WHO grade, IDH mutation status, and 1p/19q co-deletion status. In the TCGA dataset, high FAM109B expression was closely associated with higher WHO grade, IDH wild-type status, and non-co-deleted 1p/19q status (Fig. 3A). In the CGGA dataset, high FAM109B expression was associated with IDH wild-type status and non-co-deleted 1p/19q status (Supplementary Fig. 2E).

Prognostic relevance of FAM109B and establishment of clinical nomograms in LGG

Survival analysis of TCGA (Fig. 3C) and CGGA (Fig. 3F) datasets revealed that patients with high FAM109B expression had significantly worse prognosis compared to those with low FAM109B expression. The same result is found in the Gravendeel dataset (Supplementary Fig. 2C). ROC curve analysis showed that the AUC values for 1, 3, and 5-year OS in the TCGA dataset were 0.846, 0.763, and 0.663 (Fig. 3C), while the AUC values in the CGGA dataset were 0.602, 0.716, and 0.688 (Fig. 3G). Additionally, univariate Cox analysis in the TCGA dataset showed that FAM109B, age, IDH status, 1p/19q codeletion, and WHO grade were high-risk factors, while multivariate Cox analysis indicated that FAM109B is an independent prognostic factor for LGG OS [hazard ratio (HR) 1.659, 95% CI (1.045–2.636); p=0.032; Table 1]. Similarly, in the CGGA dataset, univariate Cox analysis
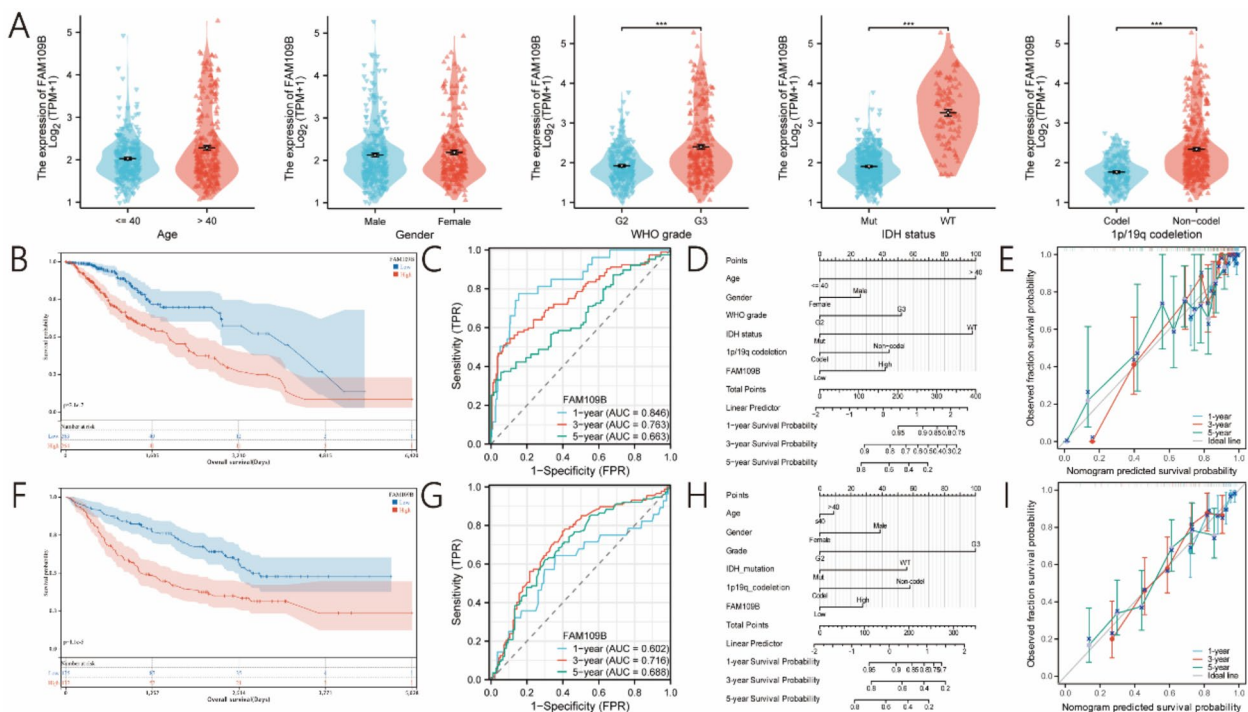

Fig. 3 Correlation and prognosis analysis of FAM109B expression with clinical features of LGG patients. **A** Correlation analysis of FAM109B expression with clinical features in the TCGA dataset. Kaplan–Meier analysis of OS in low-grade glioma patients in the TCGA (**B**) and CGGA (**F**) datasets. ROC curves of OS in the TCGA (**C**) and CGGA (**G**) datasets. Construction of a nomogram model in the TCGA (**D**) and CGGA (**H**) datasets. Calibration plot validation in the TCGA (**E**) and CGGA (**I**) datasets. *p < 0.05, **p < 0.01, and ***p < 0.001

Zhang *et al. Journal of Translational Medicine* (2024) 22:833

Page 7 of 15

Table 1 Univariate and multivariate analysis of FAM109B expression on overall survival in TCGA

Characteristics	Total (N)	Univariate analysis		Multivariate analysis	
		Hazard ratio (95% CI)	P value	Hazard ratio (95% CI)	P value
Age	530				
≤ 40	265				
> 40	265	2.898 (2.015–4.168)	< 0.001	3.238 (2.099–4.996)	< 0.001
Gender	530				
Female	238				
Male	292	1.112 (0.791–1.563)	0.542		
IDH status	527				
WT	97				
Mut	430	0.184 (0.129–0.263)	< 0.001	0.351 (0.221–0.557)	< 0.001
1p/19q codeletion	530				
Non-codel	359				
Codel	171	0.401 (0.256–0.629)	< 0.001	0.593 (0.351–1.003)	0.052
WHO grade	468				
G2	223				
G3	245	3.023 (2.022–4.519)	< 0.001	1.847 (1.184–2.879)	0.007
FAM109B	530				
Low	264				
High	266	2.652 (1.827–3.847)	< 0.001	1.659 (1.045–2.636)	0.032

showed that FAM109B, IDH status, and WHO grade were high-risk factors, and multivariate Cox analysis indicated that FAM109B is an independent prognostic factor for LGG OS [hazard ratio (HR) 0.592, 95% CI (0.404–0.867); p = 0.007; Table 2]. Thus, FAM109B is an independent factor affecting the prognosis of LGG patients. To explore the potential clinical prognostic ability of FAM109B in LGG, we established nomogram models using the TCGA (Fig. 3D) and CGGA (Fig. 3H) datasets. Calibration plots indicated that the nomogram models had high accuracy in predicting 1/3/5-year OS in LGG patients (Fig. 3E, I). These results suggest that the

Table 2 Univariate and multivariate analysis of FAM109B expression on overall survival in CGGA

Characteristics	Total (N)	Univariate analysis		Multivariate analysis	
		Hazard ratio (95% CI)	P value	Hazard ratio (95% CI)	P value
Age	257				
≤ 40	134				
> 40	123	0.894 (0.636–1.256)	0.518	0.932 (0.659–1.316)	0.687
Gender	257				
Female	112				
Male	145	1.352 (0.953–1.919)	0.091	1.677 (1.158–2.427)	0.006
IDH status	257				
WT	60				
Mut	197	0.459 (0.316–0.666)	< 0.001	0.449 (0.292–0.689)	< 0.001
WHO grade	257				
G2	96				
G3	161	0.344 (0.227–0.520)	< 0.001	0.305 (0.200–0.464)	< 0.001
FAM109B	257				
Low	130				
High	127	0.474 (0.335–0.672)	< 0.001	0.592 (0.404–0.867)	0.007

Zhang *et al. Journal of Translational Medicine*   (2024) 22:833

Page 8 of 15

established nomogram models can accurately assess the prognosis of LGG patients.

DNA methylation of FAM109B in LGG

We used the MethSurv database to analyze differential methylation of CpG islands in the promoter region of FAM109B in gliomas. We found that three methylated CpGs of FAM109B (cg17916520, cg08057985, cg16740427) decreased with the increase in tumor grade (Fig. 4A). Kaplan–Meier curves indicated that patients with high methylation of FAM109B had better prognosis compared to those with low methylation (Fig. 4B).

Functional enrichment analysis of differentially expressed genes (DEGs) associated with FAM109B expression in LGG

To analyze the molecular mechanisms associated with differential expression of FAM109B, we performed GO and KEGG enrichment analysis of DEGs screened from the TCGA and CGGA datasets. GO analysis results showed that in both the TCGA (Fig. 4C) and CGGA (Fig. 4D) datasets, DEGs were closely related to leukocyte-mediated immunity, positive regulation of leukocyte activation, immune response regulatory signaling pathways, plasma membrane signaling receptor complex, and leukocyte cell–cell adhesion. KEGG analysis results showed that in the TCGA (Fig. 4E) and CGGA (Fig. 4F) datasets, DEGs were closely related to cytokine-cytokine receptor interaction, cell adhesion molecules, PI3K-AKT, p53, IL17, and MAPK signaling pathways.

Correlation between FAM109B and immune cell infiltration and tumor microenvironment in LGG

To further investigate the potential role of FAM109B in gliomas, we used the ssGSEA algorithm to calculate the infiltration levels of 24 immune cell types in the TCGA dataset. We found that FAM109B expression was positively correlated with infiltration levels of macrophages, neutrophils, eosinophils, cytotoxic cells, and aDC, while negatively correlated with pDC (Fig. 5A, B). Using the TIMER algorithm to further estimate the infiltration of six immune cell types, we similarly found that FAM109B was positively correlated with macrophages and neutrophils (Supplementary Fig. 3A). Additionally, single-cell sequencing analysis of gliomas revealed that FAM109B was primarily expressed in macrophages (Fig. 5C). Further analysis of the correlation between FAM109B and markers of macrophage M1 (IL12A, NOS2, PTGS2, CCL3, and TNF) and macrophage M2 (TGFB1, IL10, CD163, and CSF1R) using TCGA and CGGA datasets showed that FAM109B was positively correlated with M2 markers (Fig. 5D). Next, we analyzed the relationship between FAM109B and the expression of immune checkpoints (ICs) and found that FAM109B was positively

correlated with most ICs in both the TCGA and CGGA datasets (Fig. 5E), with detailed analysis of eight key ICs (Fig. 5F, Supplementary Figure S3B). Finally, we investigated the correlation between FAM109B and chemotherapy drug sensitivity, finding that FAM109B was closely associated with lower inhibitory concentration (IC50) of common chemotherapy drugs, indicating that tumors with high FAM109B expression are more sensitive to these chemotherapy drugs (Supplementary Figure S3C, D).

Correlation between FAM109B and genomic variations in LGG

By identifying significantly altered regions of amplification or deletion in low-grade glioma patients, we found that FAM109B was negatively correlated with copy number variations (CNV) (Fig. 6A). The amplification of the gene set CNV predicted poorer prognosis compared to WT (Fig. 6B). Mutation analysis further revealed that isocitrate dehydrogenase 1 (IDH1) was the most commonly mutated gene in FAM109B expression (Fig. 6C). Kaplan–Meier curves showed that LGG patients with higher FAM109B expression and TMB levels had poorer OS (Fig. 6D).

In vitro experiments of FAM109B in LGG

Colony formation assays showed that knocking out FAM109B significantly reduced cell colonies compared to the NC group (Fig. 7A, C). EdU assays indicated that knocking out FAM109B significantly inhibited cell proliferation (Fig. 7B, D). CCK-8 assay results showed that silencing FAM109B significantly reduced the viability of SW1088 cells (Fig. 7E).

In vivo experiments of FAM109B in nude mice

To study the effect of FAM109B on glioma growth in vivo, we implanted U251 cells with stable FAM109B knockdown into nude mice to establish a tumor model. Compared to the control group, the tumors in the sh-FAM109B group mice were significantly smaller and grew slower (Fig. 7F, G). The sh-FAM109B group mice experienced slower weight loss and had longer survival times compared to the control group (Fig. 7H, I). Additionally, compared with the control group, the sh-FAM109B group showed a significant decrease in M2 macrophages (CD163) (Fig. 7J).

Discussion

Gliomas are the most common and deadliest central nervous system tumors [28]. With the advancement of science and technology, surgery and radiochemotherapy have significantly improved the survival rate of glioma patients. However, the median survival of
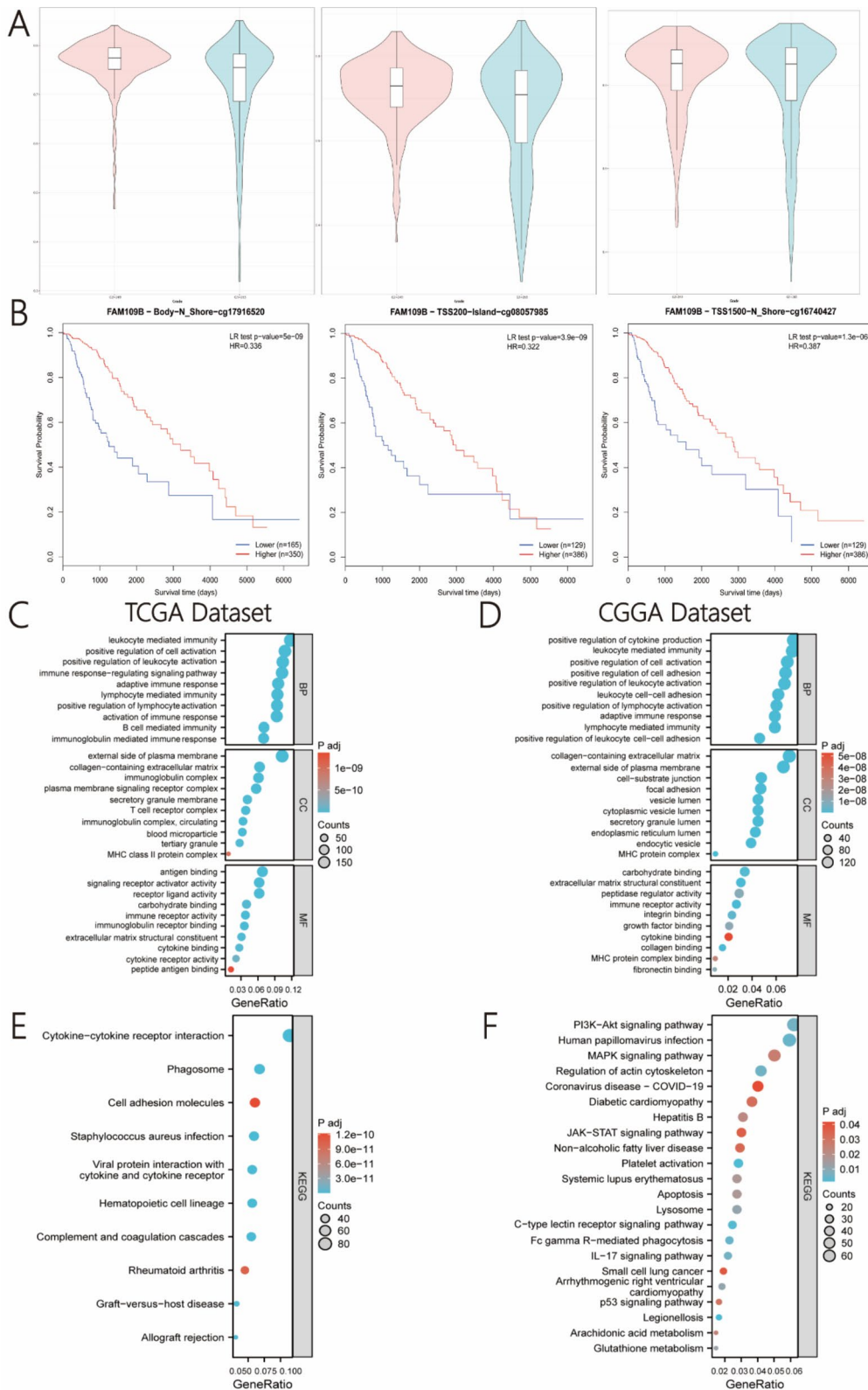
Zhang *et al. Journal of Translational Medicine*   (2024) 22:833

Page 9 of 15

Fig. 4 Methylation and functional enrichment analysis of FAM109B expression. **A** With increasing tumor grade, the methylation CpGs of FAM109B in glioma patients significantly decrease. **B** Kaplan–Meier curves show that lower methylation is associated with poorer prognosis. GO analysis of DEGs based on FAM109B expression levels in LGG patients in the TCGA (**C**) and CGGA (**D**) datasets. KEGG analysis of DEGs based on FAM109B expression levels in LGG patients in the TCGA (**E**) and CGGA (**F**) datasets
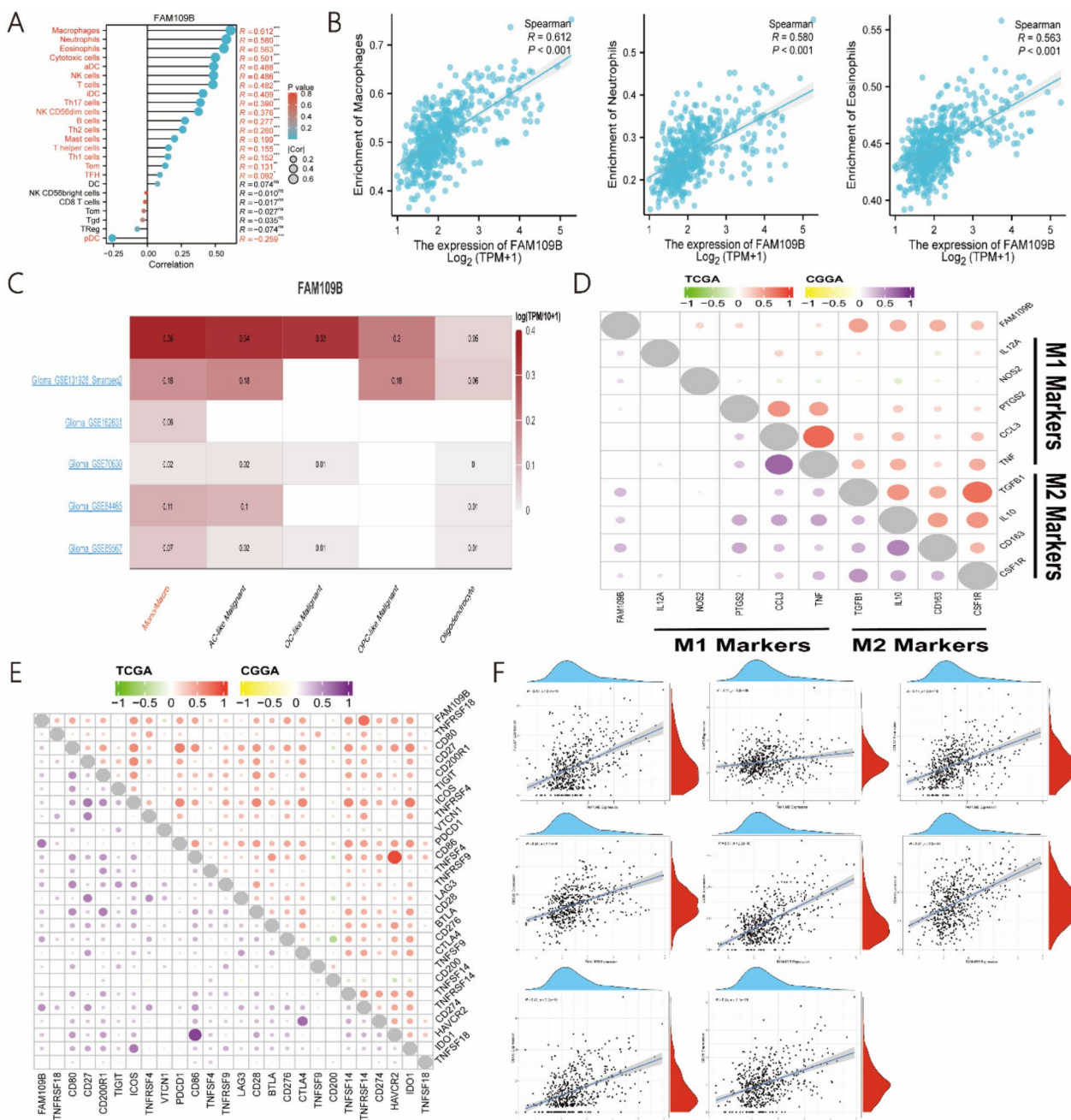
Fig. 5 Immune cell infiltration and single-cell analysis of FAM109B expression. **A** Lollipop plot showing the correlation between FAM109B expression and common immune cell infiltration. **B** Detailed analysis of the correlation between FAM109B expression and macrophages, neutrophils, and eosinophils. **C** FAM109B expression in single-cell data of glioma patients. **D** Correlation between FAM109B expression and markers of M1 and M2 macrophages in LGG patients in the TCGA and CGGA datasets. **E** Correlation between FAM109B and immune checkpoints (ICs) in LGG patients in the TCGA and CGGA datasets. **F** Detailed analysis of the correlation between FAM109B and the most common eight immune checkpoints (ICs) in LGG patients in the TCGA dataset

patients with low-grade gliomas remains poor, approximately 5–7 years. The median survival of patients with high-grade tumors is even worse, about 9–10 months [29]. Therefore, finding new and effective treatments

to improve the therapeutic outcomes and overall survival of glioma patients is crucial [30]. FAM109B has only been reported as one of the main biomarkers in breast cancer [12], and its performance in other cancers
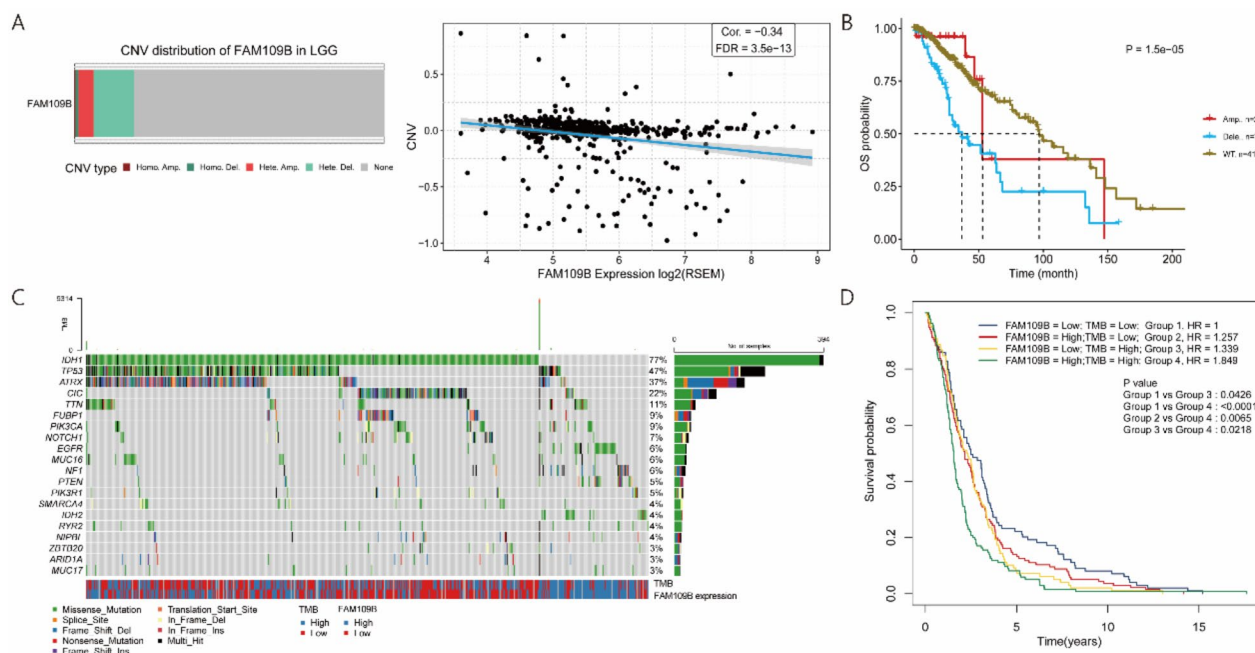
Zhang *et al. Journal of Translational Medicine* (2024) 22:833

Page 11 of 15

Fig. 6 Correlation analysis of FAM109B expression with genomic variations in LGG. **A** Correlation between FAM109B expression and copy number variations (CNV). **B** Kaplan–Meier curves show that CNV amplification is associated with poorer prognosis. **C** Waterfall plot showing the top 20 mutated genes based on FAM109B expression. **D** Kaplan–Meier curves showing the prognostic differences between high and low FAM109B expression groups with different TMB levels

is unclear. Its role in the pathophysiological development of central nervous system tumors is also unknown. In this study, we fully utilized transcriptomic data from the TCGA and CGGA databases to show through pancancer analysis that FAM109B is upregulated in 19 tumor types and significantly elevated in low-grade gliomas. FAM109B is closely associated with macrophages and higher TMB. Univariate Cox regression analysis showed that FAM109B expression is significantly associated with poor prognosis in BLCA, LAML, LGG, and MESO. Thus, FAM109B plays a crucial role in multiple tumor types, making it imperative to explore its potential role in tumors.

To investigate the role of FAM109B in gliomas, we analyzed data from the TCGA, CGGA, and HPA databases, finding that FAM109B expression in glioma tissues was significantly higher than in normal tissues at both the transcript and protein levels. Clinical studies on tissue samples from patients with low-grade gliomas

also showed high expression of FAM109B in low-grade gliomas. Univariate and multivariate Cox regression analyses indicated that FAM109B is an independent prognostic factor for LGG patients. Based on the Cox regression analysis results, we constructed a clinical nomogram model to predict the 1-, 3-, and 5-year OS of LGG patients and validated its accuracy using calibration curves. Additionally, FAM109B expression significantly increased with tumor grade and was considerably correlated with the clinical characteristics of LGG patients. DNA methylation plays an essential role in complex diseases and is crucial for interactions between tumors and immune cells [31]. Analysis of FAM109B promoter methylation showed that FAM109B methylation CpGs decreased with increasing tumor grade, and low methylation was associated with poorer prognosis. FAM109B DNA methylation might also regulate its expression and influence the prognosis of glioma patients. Finally, in vitro studies showed that silencing FAM109B

(See figure on next page.)

Fig. 7 Validation analysis of FAM109B expression in vitro and in vivo experiments. Effects of FAM109B knockout on colony formation of SW1088 cells (**A**) and statistical analysis (**C**). Representative images of EdU assay (**B**) and statistical analysis (**D**) after FAM109B knockout in SW1088 cells. **E** Cell viability of SW1088 cells in the sh-NC and sh-FAM109B groups detected by CCK-8 assay. In vivo bioluminescence imaging (**G**) and statistical analysis (**F**) on days 0, 7, 14, and 21 from the sh-NC and sh-FAM109B groups infected with lentivirus. Weight (**H**) and Kaplan–Meier survival analysis (**I**) of nude mice. **J** M2 macrophages in tumor lesions of both groups were detected using CD163 immunostaining. The magnification was ×20. *$p < 0.05$, **$p < 0.01$, and ***$p < 0.001$

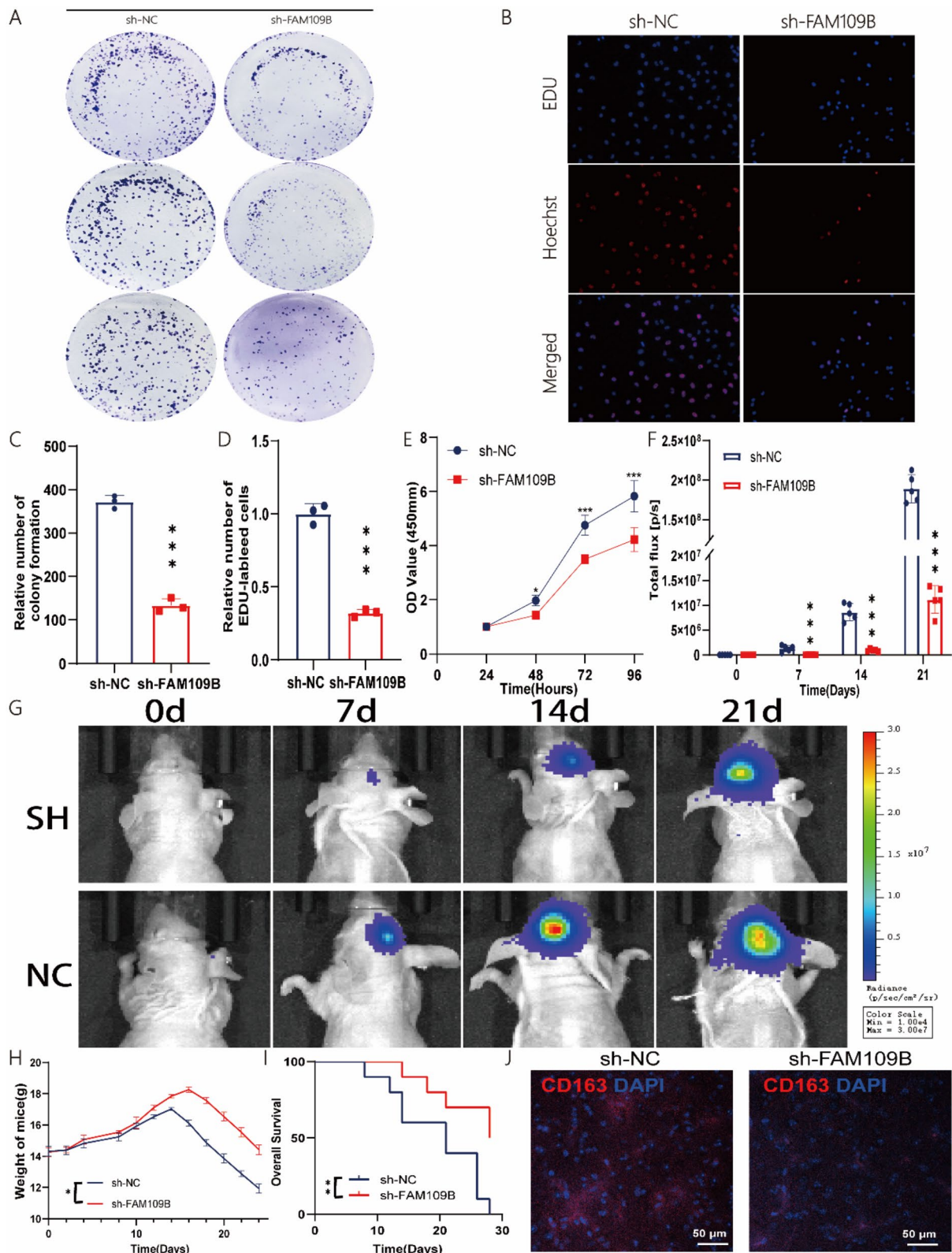**Fig. 7** (See legend on previous page.)

Zhang *et al. Journal of Translational Medicine*   (2024) 22:833

Page 13 of 15

expression significantly reduced the proliferation capacity of LGG cells. In vivo studies demonstrated that silencing FAM109B expression significantly inhibited glioma growth, confirming the critical role of FAM109B in glioma cell proliferation. In summary, FAM109B is involved in more aggressive biological processes in gliomas, and studying its potential role in glioma pathogenesis and validating it as a potential biomarker for LGG is meaningful.

The tumor microenvironment (TME) consists of various immune cell types and plays a crucial role at every stage of tumor initiation, progression, invasion, intravasation, metastatic dissemination, and growth, as well as in the development of chemoresistance [32–34]. Tumor-associated macrophages (TAMs) are a vital component of the TME and represent the most abundant type of tumor-infiltrating immune cells [35, 36]. TAMs are associated with microvessel density in tumor tissues and play important roles in tumor progression, immune suppression, invasion, and metastasis [37, 38]. TAMs are generally categorized into M1-type macrophages (M1) and M2-type macrophages (M2). M1 macrophages release tumor-killing molecules (such as ROS and NO) and exhibit cytotoxic effects on tumor cells [39, 40]. In contrast, M2 macrophages suppress T-cell-mediated anti-tumor immune responses, promote tumor angiogenesis, and facilitate tumorigenesis and metastasis [37, 41]. In this study, we found that FAM109B is closely related to the immune functions of TAMs in LGG. Analyzing the potential biological functions of FAM109B revealed that DEGs are significantly associated with processes such as leukocyte-mediated immunity, regulation of immune response signaling pathways, plasma membrane signal receptor complexes, and leukocyte-cell adhesion, as well as pathways like cytokine-cytokine receptor interaction, PI3K-AKT, MAPK, and p53. Single-cell analysis of gliomas indicated that FAM109B expression is primarily associated with macrophages. TIMER and ssGSEA algorithm analyses demonstrated a positive correlation between FAM109B and macrophages in low-grade gliomas. Additionally, in the TCGA and CGGA databases, FAM109B was positively correlated with M2 macrophage markers. Thus, the immune role of FAM109B in low-grade gliomas may be attributed to TAMs. TAM infiltration is closely associated with poor prognosis in cancer patients, and targeting TAMs is a potentially attractive therapeutic strategy [35].

Genomic variations play a critical role in tumor immune infiltration and prognosis [42, 43]. Through somatic mutation analysis detecting genetic variations, we found that IDH1 is the most common mutated gene in FAM109B expression, while isocitrate dehydrogenase 1 (IDH1) is the most frequently mutated gene in WHO grade II–III gliomas [44]. The mutation of IDH1 is crucial for the diagnosis and treatment of gliomas, and genomic variations appear to influence FAM109B gene expression and prognosis, indicating significant functional implications. Immunotherapy holds great promise for LGG patients, but its progress in gliomas remains challenging [45]. Immune checkpoint inhibitors (ICIs) inhibit tumor cell growth by enhancing anti-tumor activity, bringing revolutionary changes and vast prospects for cancer treatment [46, 47]. We found that FAM109B is positively correlated with common immune checkpoints (ICs), suggesting that FAM109B has potential as a targeted inhibitor for cancer therapy. Temozolomide (TMZ) is widely used for treating gliomas, but its efficacy is often limited by resistance [48]. We found that FAM109B is highly sensitive to PLK1 inhibitors (BI-2536, GSK461364), PI3K and mTOR inhibitors (PI-103), non-lipid ceramidase inhibitors (ceranib-2), FAAH inhibitors (LY2183240), chemokine receptor CXCR2 non-peptide antagonists (SB225002), MET receptor tyrosine kinase inhibitors (Tivantinib), HDAC inhibitors (AR-42), HDAC6 inhibitors (CAY10603), and HDAC inhibitors (Tubastatin A), suggesting that FAM109B may be a potential predictor of chemosensitivity in LGG patients.

This study proposes that FAM109B becomes a new prognostic biomarker in low-grade gliomas and is a promising immunotherapeutic target, providing new indicators for individualized precision treatment of patients. Our study has certain limitations. First, we did not thoroughly investigate the role of FAM109B in high-grade gliomas to confirm that FAM109B is a reliable immunotherapeutic target for glioma patients. Second, we did not verify the specific expression of FAM109B in M2-like macrophages and the experiments related to FAM109B-induced M2-like macrophage polarization. These limitations will guide our future research directions.

Conclusions

FAM109B is significantly upregulated in various tumor tissues and is associated with poor prognosis. As a new prognostic biomarker for LGG, FAM109B may be a potential therapeutic target for LGG patients. FAM109B shows specific overexpression in TAMs and is closely related to the immunological characteristics of low-grade gliomas.

Zhang *et al. Journal of Translational Medicine*   (2024) 22:833

Page 14 of 15

Supplementary Information

Author contributions
ZZ, YX and SYZ contributed equally to this work. The experimental conception and design were completed by ZZ, YX and HG. Experimental data were downloaded and analyzed by JZ and BL. Clinical samples and data were collected by SYZ and XSS. Review and editing was done by JL and FX. The manuscript was co-authored by ZZ, HZ, and HG, and was reviewed by all authors. All authors read and approved the final manuscript.

Availability of data and materials
The TCGA glioma data used to support the analysis in this study were downloaded from TCGA (http://portal.gdc.cancer.gov). The CGGA glioma data used in this study to support the analysis can be downloaded from CGGA (http://www.cgga.org.cn/). The Gravendeel glioma data used to support analysis are available from Gliovis (http://gliovis.bioinfo.cnio.es) to download.

Declarations

Ethics approval and consent to participate
This study was approved by the Ethics Review Committee of the Second Affiliated Hospital of Nanchang University (Project approval ID: O-Medical Research Ethics Review [2024] No. 21).

Competing interests
The authors declare that they have no known competing financial interests or personal relationships that could have appeared to influence the work reported in this article.

Author details
[1]Department of Neurosurgery, The Second Affiliated Hospital, Jiangxi Medical College, Nanchang University, Jiangxi, China. [2]Institute of Neuroscience, Nanchang University, Jiangxi, China. [3]Jiangxi Province Key Laboratory of Neurological Diseases, Jiangxi, China. [4]JXHC Key Laboratory of Neurological Medicine, Jiangxi, China.

References
1. Guerreiro Stucklin AS, Ryall S, Fukuoka K, Zapotocky M, Lassaletta A, Li C, Bridge T, Kim B, Arnoldo A, Kowalski PE, Zhong Y, Johnson M, Li C, Ramani AK, Siddaway R, Nobre LF, de Antonellis P, Dunham C, Cheng S, Boué DR, Finlay JL, Coven SL, de Prada I, Perez-Somarriba M, Faria CC, Grotzer MA, Rushing E, Sumerauer D, Zamecnik J, Krskova L, Garcia Ariza M, Cruz O, Morales La Madrid A, Solano P, Terashima K, Nakano Y, Ichimura K, Nagane M, Sakamoto H, Gil-da-Costa MJ, Silva R, Johnston DL, Michaud J, Wilson B, van Landeghem FKH, Oviedo A, McNeely PD, Crooks B, Fried I, Zhukova N, Hansford JR, Nageswararao A, Garzia L, Shago M, Brudno M, Irwin MS, Bartels U, Ramaswamy V, Bouffet E, Taylor MD, Tabori U, Hawkins C. Alterations in ALK/ROS1/NTRK/MET drive a group of infantile hemispheric gliomas. Nat Commun. 2019;10:4343.
2. Ostrom QT, Gittleman H, Xu J, Kromer C, Wolinsky Y, Kruchko C, Barnholtz-Sloan JS. CBTRUS statistical report: primary brain and other central nervous system tumors diagnosed in the United States in 2009–2013. Neuro Oncol. 2016;18:v1–75.
3. Jin Z, Piao L, Sun G, Lv C, Jing Y, Jin R. Long non-coding RNA PART1 exerts tumor suppressive functions in glioma via sponging miR-190a-3p and inactivation of PTEN/AKT pathway. Onco Targets Ther. 2020;13:1073–86.
4. Gahoi N, Syed P, Choudhary S, Epari S, Moiyadi A, Varma SG, Gandhi MN, Srivastava S. A protein microarray-based investigation of cerebrospinal fluid reveals distinct autoantibody signature in low and high-grade gliomas. Front Oncol. 2020;10: 543947.
5. Akkus Z, Ali I, Sedlář J, Agrawal JP, Parney IF, Giannini C, Erickson BJ. Predicting deletion of chromosomal arms 1p/19q in low-grade gliomas from MR images using machine intelligence. J Digit Imaging. 2017;30:469–76.
6. Teng C, Zhu Y, Li Y, Dai L, Pan Z, Wanggou S, Li X. Recurrence- and malignant progression-associated biomarkers in low-grade gliomas and their roles in immunotherapy. Front Immunol. 2022;13: 899710.
7. Doucette T, Latha K, Yang Y, Fuller GN, Rao A, Rao G. Survivin transcript variant 2 drives angiogenesis and malignant progression in proneural gliomas. Neuro Oncol. 2014;16:1220–8.
8. Elkin SR, Lakoduk AM, Schmid SL. Endocytic pathways and endosomal trafficking: a primer. Wien Med Wochenschr. 1946;166(2016):196–204.
9. Pineda-Cirera L, Cabana-Domínguez J, Lee PH, Fernàndez-Castillo N, Cormand B. Identification of genetic variants influencing methylation in brain with pleiotropic effects on psychiatric disorders. Prog Neuropsychopharmacol Biol Psychiatry. 2022;113: 110454.
10. Mustafin RN, Kazantseva AV, Enikeeva RF, Malykh SB, Khusnutdinova EK. Longitudinal genetic studies of cognitive characteristics. Vavilovskii zhurnal genetiki i selektsii. 2020;24:87–95.
11. Swan LE, Tomasini L, Pirruccello M, Lunardi J, De Camilli P. Two closely related endocytic proteins that share a common OCRL-binding motif with APPL1. Proc Natl Acad Sci USA. 2010;107:3511–6.
12. Mehmood A, Nawab S, Jin Y, Hassan H, Kaushik AC, Wei DQ. Ranking breast cancer drugs and biomarkers identification using machine learning and pharmacogenomics. ACS Pharmacol Transl Sci. 2023;6:399–409.
13. Li M, Shi P, Yang H, Liu S, Sun R, Li L, Zhao Z, Sun J. The immune cells have complex causal regulation effects on cancers. Int Immunopharmacol. 2024;134: 112179.
14. Hoogstrate Y, Draaisma K, Ghisai SA, van Hijfte L, Barin N, de Heer I, Coppieters W, van den Bosch TPP, Bolleboom A, Gao Z, Vincent A, Karim L, Deckers M, Taphoorn MJB, Kerkhof M, Weyerbrock A, Sanson M, Hoeben A, Lukacova S, Lombardi G, Leenstra S, Hanse M, Fleischeuer REM, Watts C, Angelopoulos N, Gorlia T, Golfinopoulos V, Bours V, van den Bent MJ, Robe PA, French PJ. Transcriptome analysis reveals tumor microenvironment changes in glioblastoma. Cancer Cell. 2023;41:678-692.e677.
15. Braun DA, Street K, Burke KP, Cookmeyer DL, Denize T, Pedersen CB, Gohil SH, Schindler N, Pomerance L, Hirsch L, Bakouny Z, Hou Y, Forman J, Huang T, Li S, Cui A, Keskin DB, Steinharter J, Bouchard G, Sun M, Pimenta EM, Xu W, Mahoney KM, McGregor BA, Hirsch MS, Chang SL, Livak KJ, McDermott DF, Shukla SA, Olsen LR, Signoretti S, Sharpe AH, Irizarry RA, Choueiri TK, Wu CJ. Progressive immune dysfunction with advancing disease stage in renal cell carcinoma. Cancer Cell. 2021;39:632-648.e638.
16. NavarroGonzalez J, Zweig AS, Speir ML, Schmelter D, Rosenbloom KR, Raney BJ, Powell CC, Nassar LR, Maulding ND, Lee CM, Lee BT, Hinrichs AS, Fyfe AC, Fernandes JD, Diekhans M, Clawson H, Casper J, Benet-Pagès A, Barber GP, Haussler D, Kuhn RM, Haeussler M, Kent WJ. The UCSC genome browser database: 2021 update. Nucleic Acids Res. 2021;49:D1046–57.
17. Liu X, Li Y, Qian Z, Sun Z, Xu K, Wang K, Liu S, Fan X, Li S, Zhang Z, Jiang T, Wang Y. A radiomic signature as a non-invasive predictor of progression-free survival in patients with lower-grade gliomas. NeuroImage Clin. 2018;20:1070–7.
18. Bowman RL, Wang Q, Carro A, Verhaak RG, Squatrito M. GlioVis data portal for visualization and analysis of brain tumor expression datasets. Neuro Oncol. 2017;19:139–41.
19. Thul PJ, Lindskog C. The human protein atlas: a spatial map of the human proteome. Protein Sci. 2018;27:233–44.
20. Modhukur V, Iljasenko T, Metsalu T, Lokk K, Laisk-Podar T, Vilo J. MethSurv: a web tool to perform multivariable survival analysis using DNA methylation data. Epigenomics. 2018;10:277–88.

21. Ritchie ME, Phipson B, Wu D, Hu Y, Law CW, Shi W, Smyth GK. limma powers differential expression analyses for RNA-sequencing and microarray studies. Nucleic Acids Res. 2015;43: e47.
22. Li T, Fan J, Wang B, Traugh N, Chen Q, Liu JS, Li B, Liu XS. TIMER: a web server for comprehensive analysis of tumor-infiltrating immune cells. Can Res. 2017;77:e108–10.
23. Hänzelmann S, Castelo R, Guinney J. GSVA: gene set variation analysis for microarray and RNA-seq data. BMC Bioinform. 2013;14:7.
24. Bindea G, Mlecnik B, Tosolini M, Kirilovsky A, Waldner M, Obenauf AC, Angell H, Fredriksen T, Lafontaine L, Berger A, Bruneval P, Fridman WH, Becker C, Pagès F, Speicher MR, Trajanoski Z, Galon J. Spatiotemporal dynamics of intratumoral immune cells reveal the immune landscape in human cancer. Immunity. 2013;39:782–95.
25. Sun D, Wang J, Han Y, Dong X, Ge J, Zheng R, Shi X, Wang B, Li Z, Ren P, Sun L, Yan Y, Zhang P, Zhang F, Li T, Wang C. TISCH: a comprehensive web resource enabling interactive single-cell transcriptome visualization of tumor microenvironment. Nucleic Acids Res. 2021;49:D1420-d1430.
26. Liu CJ, Hu FF, Xie GY, Miao YR, Li XW, Zeng Y, Guo AY. GSCA: an integrated platform for gene set cancer analysis at genomic, pharmacogenomic and immunogenomic levels. Brief Bioinform. 2023;24: bbac558.
27. Liu CJ, Hu FF, Xia MX, Han L, Zhang Q, Guo AY. GSCALite: a web server for gene set cancer analysis. Bioinformatics. 2018;34:3771–2.
28. Zamler DB, Hu J. Primitive oligodendrocyte precursor cells are highly susceptible to gliomagenic transformation. Can Res. 2023;83:807–8.
29. Kannan S, Murugan AK, Balasubramanian S, Munirajan AK, Alzahrani AS. Gliomas: genetic alterations, mechanisms of metastasis, recurrence, drug resistance, and recent trends in molecular therapeutic options. Biochem Pharmacol. 2022;201: 115090.
30. Lowenstein PR, Baker GJ, Castro MG. Cracking the glioma-NK inhibitory code: toward successful innate immunotherapy. Oncoimmunology. 2014;3: e965573.
31. Cao J, Yan Q. Cancer epigenetics, tumor immunity, and immunotherapy. Trends Cancer. 2020;6:580–92.
32. de Visser KE, Joyce JA. The evolving tumor microenvironment: from cancer initiation to metastatic outgrowth. Cancer Cell. 2023;41:374–403.
33. Seebacher NA, Krchniakova M, Stacy AE, Skoda J, Jansson PJ. Tumour microenvironment stress promotes the development of drug resistance. Antioxidants. 2021;10:1801.
34. DeNardo DG, Ruffell B. Macrophages as regulators of tumour immunity and immunotherapy. Nat Rev Immunol. 2019;19:369–82.
35. Chen Y, Song Y, Du W, Gong L, Chang H, Zou Z. Tumor-associated macrophages: an accomplice in solid tumor progression. J Biomed Sci. 2019;26:78.
36. Zhou K, Cheng T, Zhan J, Peng X, Zhang Y, Wen J, Chen X, Ying M. Targeting tumor-associated macrophages in the tumor microenvironment. Oncol Lett. 2020;20:234.
37. Pan Y, Yu Y, Wang X, Zhang T. Tumor-associated macrophages in tumor immunity. Front Immunol. 2020;11: 583084.
38. Cheng K, Cai N, Zhu J, Yang X, Liang H, Zhang W. Tumor-associated macrophages in liver cancer: from mechanisms to therapy. Cancer Commun. 2022;42:1112–40.
39. Bernsmeier C, van der Merwe S, Périanin A. Innate immune cells in cirrhosis. J Hepatol. 2020;73:186–201.
40. Xu Y, Cui K, Li J, Tang X, Lin J, Lu X, Huang R, Yang B, Shi Y, Ye D, Huang J, Yu S, Liang X. Melatonin attenuates choroidal neovascularization by regulating macrophage/microglia polarization via inhibition of RhoA/ROCK signaling pathway. J Pineal Res. 2020;69: e12660.
41. Annamalai RT, Turner PA, Carson WFT, Levi B, Kunkel S, Stegemann JP. Harnessing macrophage-mediated degradation of gelatin microspheres for spatiotemporal control of BMP2 release. Biomaterials. 2018;161:216–27.
42. Braun DA, Hou Y, Bakouny Z, Ficial M, Sant' Angelo M, Forman J, Ross-Macdonald P, Berger AC, Jegede OA, Elagina L, Steinharter J, Sun M, Wind-Rotolo M, Pignon JC, Cherniack AD, Lichtenstein L, Neuberg D, Catalano P, Freeman GJ, Sharpe AH, McDermott DF, Van Allen EM, Signoretti S, Wu CJ, Shukla SA, Choueiri TK. Interplay of somatic alterations and immune infiltration modulates response to PD-1 blockade in advanced clear cell renal cell carcinoma. Nat Med. 2020;26:909–18.
43. Fujita M, Yamaguchi R, Hasegawa T, Shimada S, Arihiro K, Hayashi S, Maejima K, Nakano K, Fujimoto A, Ono A, Aikata H, Ueno M, Hayami S, Tanaka H, Miyano S, Yamaue H, Chayama K, Kakimi K, Tanaka S, Imoto S, Nakagawa H. Classification of primary liver cancer with immunosuppression

mechanisms and correlation with genomic alterations. EBioMedicine. 2020;53: 102659.
44. Philip B, Yu DX, Silvis MR, Shin CH, Robinson JP, Robinson GL, Welker AE, Angel SN, Tripp SR, Sonnen JA, VanBrocklin MW, Gibbons RJ, Looper RE, Colman H, Holmen SL. Mutant IDH1 promotes glioma formation in vivo. Cell Rep. 2018;23:1553–64.
45. Zhou J, Guo H, Liu L, Jin Z, Zhang W, Tang T. Identification of immune-related hub genes and construction of an immune-related gene prognostic index for low-grade glioma. J Cell Mol Med. 2023;27:3851–63.
46. Yin J, Song Y, Tang J, Zhang B. What is the optimal duration of immune checkpoint inhibitors in malignant tumors? Front Immunol. 2022;13: 983581.
47. Shi MY, Liu HG, Chen XH, Tian Y, Chen ZN, Wang K. The application basis of immuno-checkpoint inhibitors combined with chemotherapy in cancer treatment. Front Immunol. 2022;13:1088886.
48. Yan Y, Xu Z, Dai S, Qian L, Sun L, Gong Z. Targeting autophagy to sensitive glioma to temozolomide treatment. J Exp Clin Cancer Res. 2016;35:23.

Publisher's Note